NASA TT F-11,797

# AN EXPERIMENTAL INVESTIGATION OF THE EFFECT OF MACH AND REYNOLDS NUMBERS ON THE STRUCTURE OF A SUPERSONIC RAREFIED GAS FLOW IN THE STAGNATION REGION OF A BLUNT BODY

A. V. Ivanov

Translation of "Eksperimental'noye Issledovaniye Vliyaniya Chisel Makha i Reynol'dsa na Strukturu Sverkhzvukovogo Potoka Razrezhennogo Gaza v Okrestnosti Peredney Kriticheskoy Tochki Zatuplennogo Tela"
Izvestiya Akademii Nauk SSSR, Mekhanika zhidkosti i Gaza, No. 3, pp. 108-115, 1967



NATIONAL AERONAUTICS AND SPACE ADMINISTRATION
WASHINGTON, D.C. 20546 JULY 1968

# AN EXPERIMENTAL INVESTIGATION OF THE EFFECT OF MACH AND REYNOLDS NUMBERS ON THE STRUCTURE OF A SUPERSONIC RAREFIED GAS FLOW IN THE STAGNATION REGION OF A BLUNT BODY

A. V. Ivanov

ABSTRACT. The effects of Mach and Reynolds numbers on the structure of a supersonic rarefied gas flow in the stagnation region of a blunt body are experimentally investigated. The electron beam method which utilizes the attenuation of an electron beam for the determination of density fields in the stagnation region of a disk and a sphere is used here in cases of various low-density flow regimes. Three series of measurements were conducted. The analysis of the results shows: (1) the increase in shock wave thickness with the decrease of density leads to the occurrence of relaxation effects in the compressed gas layer ahead of a body; (2) with a further decrease in density the shock wave vanishes and the flow becomes a free-molecular flow; (3) the ratio of the shock-detachment distance $\Delta$ to the length of a free path $\lambda_\infty$ in a free flow may be considered as the flow criterion for flow regimes taking place prior to disappearance of the shock wave. However, the number of collisions experienced by a certain molecule in passing through a disturbed layer ahead of a body appears to be a more rigorous criterion.

The use of the scattering of electrons from a collimated beam by gas molecules present in the tested space makes it possible to determine the field of local densities in the flow of a rarefied gas [1, 2]. This method has been used to show that [2] when a blunt body is in a low-density supersonic air flow the flow structure in front of the blunt body differs substantially from that of continuum flow. In particular it was established that a significant portion of the perturbed region in front of the body in the flow is filled with a spread shock wave. According to measurements [2-5] the thickness d of the latter is several mean free paths $\lambda_\infty$ in the incident flow, which is substantially greater than the length of the mean free path $\lambda_s$ behind a normal shock. This shows that the estimates of Probstein [6], which are based on the proposition that $d \approx \lambda_s$, are incorrect. /108[1]

If the experimental value of $d \approx \lambda_\infty$ is used, the comparison of boundary layer thickness $\delta$ and shock wave thickness d leads to the conclusion that the thickness d must not be disregarded during the flow transition state. Furthermore the thickness of the shock wave increases more rapidly than the thickness

[1]Numbers in the margin indicate pagination in the foreign text.

of the boundary layer when the density of the incident flow is reduced. Consequently it should be expected that, at some moment of time, d and $\delta$ will both be comparable to the value of the shock wave departure $\Delta$ from the body in continuum flow. The state of the gas in the vicinity of the frontal stagnation point on the blunt body must, in this case, depend on the physical processes which occur in the shock wave and the flow mechanism is indeed more complex than that of the model proposed in [6].

| Model | $r^\circ$ мм | $M$ | $R_\infty$ | $\lambda_\infty$ мм | $\Delta\lambda_\infty$ |
|---|---|---|---|---|---|
| 1 Disk | 7.5 | | 52 | 0.82 | 5.14 |
| | 7.5 | 3.75—3.8 | 35 | 1.2 | 3.56 |
| | 5 | | 24 | 1.2 | 2.37 |
| | 2.5 | | 12 | 1.2 | 1.19 |
| 2 Sphere | 7.5 | | 100 | 0.4 | 3.3 |
| | 7.5 | 3.7—3.8 | 52 | 0.82 | 1.65 |
| | 7.5 | | 35 | 1.2 | 1.17 |
| 3 Sphere | 7.5 | 2.6 | | 0.33 | 6 |
| | 7.5 | 3.7 | 90—100 | 0.4 | 3.9 |
| | 5.3 | 5.8 | | 0.5 | 2.34 |

The density fields in front of a circular disk and a sphere were measured experimentally in our work for different flow states in order to investigate the variation in the nature of flow past a blunt body when the density of the incident flow is reduced. The temperature of the model was approximately equal /109 to the stagnation temperature and consequently the simulating conditions were those for flow around a thermally insulated body. The Knudsen number was varied by varying the Mach number M and the Reynolds number $R_\infty$.

Three series of measurements were carried out. In the first two series which were for a disk and a sphere respectively, we investigated the variation in the flow picture when the Reynolds number was varied while the Mach number was held constant at M = 3.7-3.8. In the third series of measurements, involving the flow around the sphere, the Reynolds number was kept constant, $R_\infty$ = 90-100, while the Mach number was varied in the range $2.6 \leqslant M \leqslant 5.8$. The table shows the specific parameters for each of the experiments in the series.

The Reynolds number $R_\infty$ was computed relative to the conditions of incident flow and body radius $r^\circ$. The Lennard-Jones molecular model [7] was used when the coefficient of viscosity and the mean free path were determined.

Experiments were conducted in a low-density wind tunnel [8]. The Mach number M was determined by measuring the total pressure head with an attachment [8]. The isentropic care of the rarefied supersonic flow had a dimension of 20 to 25 mm in all cases. The air in the receiver was at room temperature in all cases.

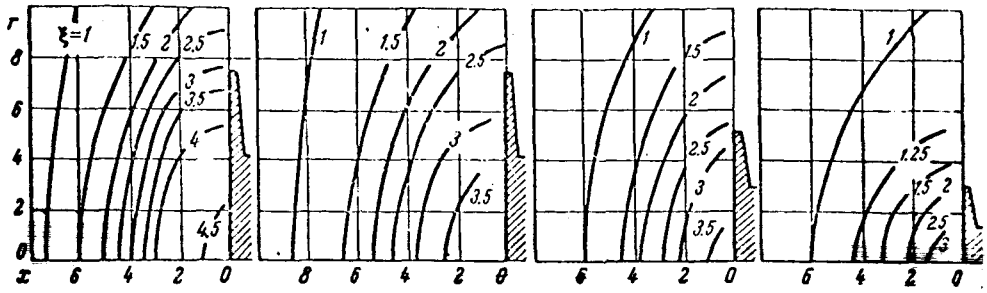


a

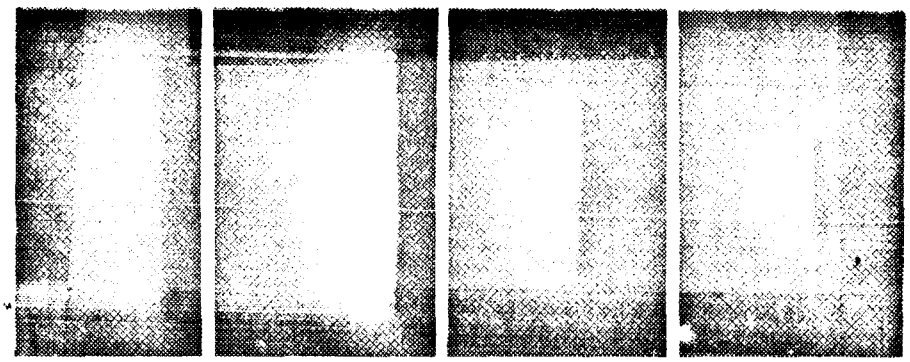

b

Figure 1. Density Fields and the Representation of Flow in Front of the Disk when M = 3.75-3.8; $R_\infty$ = 52, 35, 24, 12.

The density fields were determined with the aid of an electron probe [1, 2]. The basic components of the apparatus [2] were the electron gun and electron detector (Faraday cylinder), installed on both sides of the axisymmetric gas flow on a common coordinate setting device which was thus capable of moving the source-detector system along the axis of the nozzle (along the x axis) as well as up and down (along the y axis). The electron beam which passed perpendicular to the gas flow (the z axis) was scattered by the molecules of this flow and the detector recorded only those electrons which passed through without a "noticeable" deflection. The aperture angle of the detector was on the order of $10^{-3}$ rad. The three-dimensional resolution of the method was 0.25 mm. The measurement process consisted of finding the distribution of electron beam intensity I(x, y) recorded by the detector as a function of the coordinate y at some cross section x of the investigated axisymmetric flow. The distribution of local density $\rho(r, x)$ for this cross section as a function of distance r from the flow axis was determined after the /110 numerical integration of expression [1, 2].

$$\rho(r, x) = \rho_\infty + \frac{1}{\pi\mu}\int_r^\infty \frac{d\ln I(x, y)}{dy}\frac{dy}{\sqrt{y^2 - r^2}} \qquad (1)$$

in which $\rho_s$ is the density outside the flow in the unperturbed region of the wind tunnel pressure chamber, $\mu$ is the mass attenuation coefficient of the electron beam.

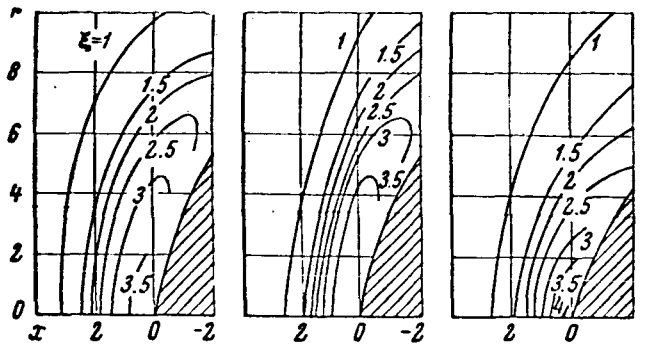


a

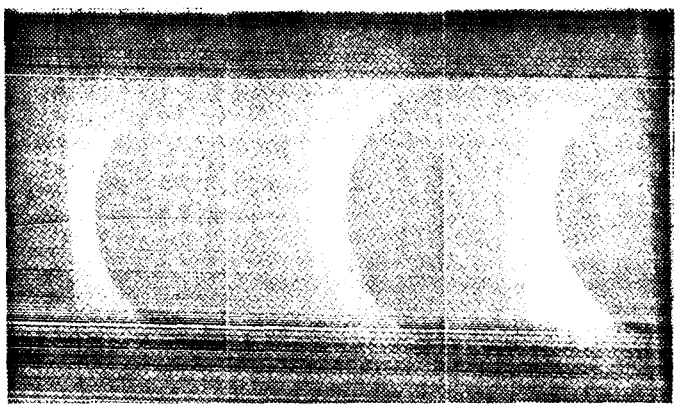

b

**Figure 2.** The Density Field and the Visualization of Flow in Front of a Sphere when M = 3.7-3.8; $R_\infty$ = 100, 52, 35.

Expression (1) follows from the attenuation law [9] for the electron beam current recorded by a detector with a narrow aperture. In the case of homogeneous distribution of density in the test space this law has the form

$$\ln I - \ln I_0 = -\mu\rho L \qquad (2)$$

where $I_0$ is the intensity of the electron beam at the output from the source when L is the distance between the source and the detector. This attenuation law is satisfied quite well when distance L does not significantly exceed the mean free path of electrons in the investigated gas [1], i.e., when $\mu\rho L \leq 1$.

In our experiments the best sensitivity of the method was provided by selecting parameters such that the condition $\mu\rho L \approx 1$ was satisfied. This was achieved by varying the quantity $\mu$. This, in turn, was achieved by varying the energy of the electron beam. Expression (2) was used to determine the attenuation coefficient from attenuation measurements on the electron beam in the chamber with air at rest whose temperature was constant and whose pressure was varied. The linear relationship between In I and the pressure p has shown that the attenuation law (2) is applicable. This relationship was established during measurements up to pressures for which distance L between the source and the detector was several mean free electron paths in the investigated gas. Measurements of coefficient $\mu$ for air were carried out in the range of energies /111 from 1 to 3 kev and showed that, for the given equipment geometry, the variation in $\mu$ as a function of accelerating voltage V is well described by the relationship $\mu = 7.75 \times 10^8 V^{-0.75}$ cm$^2$/g (V, in volts).

The maximum error incurred when the density was determined by means of equation (1) was 10 to 15%.

The distribution I (x, y) was measured at a sufficiently removed distance up along the flow from the blunt body. This made it possible to determine the density distribution $\rho(r, x_\infty)$ in the unperturbed incident flow. The value of the density $\rho_\infty$ in the unperturbed isentropic care of the flow, established via the above method, was compared with the value computed from the experimental M number. It was shown that the results obtained by the two different methods were in good agreement.

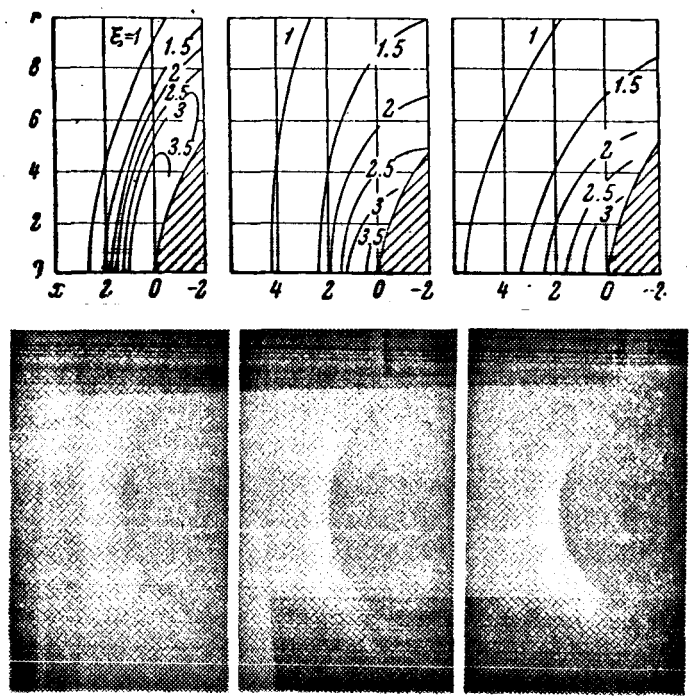


Figure 3. Density Fields and Flow Visualization in Front of the Sphere for $R_\infty$ = 90-100; M = 2.6, 3.7, 5.8.

Figures 1-3 show equal density lines $\xi = \rho/\rho_\infty$ in the vicinity of the frontal critical point of the blunt body for the three series of experiments described in the table. The order of flow pictures arrangement for different M and $R_\infty$ is the same as in the table and corresponds to an increase in the Knudsen number from the left to the right. The distances are plotted along the coordinate axes in millimeters. These figures show photographs of the flow obtained by the glow discharge method [10], in the same order, for the purpose of their qualitative comparison with experimental density fields.

Figures 1-3 can be used to trace the increase in the dimension of the perturbed region in front of the body as the incident flow becomes more rarefied. In the case of continuum flow the value of the perturbed region in front of the blunt body is equal to continuum departure $\Delta$ of the shock wave. In free molecular flow it is determined by the mean free path of molecules reflected from the body in the incident field [11]. It is obvious that this region increases as the gas density decreases.

The results shown in Figures 1-3 pertain to the transition state of the flow when the mechanism of continuum flow gradually transforms into the mechanism of discrete collisions.

The relative density profiles $\xi = \rho/\rho_\infty$ along the flow axis are shown in Figures 4-6 for flows around blunt bodies investigated in this work.

In addition to experimental curves, these figures also show the position /112
of the detached shock wave during continuum flow. It is clear from these figures that in addition to an increase in the dimension of the perturbed region, the increase in the Knudsen number $\lambda_\infty/r^\circ$ is accompanied by a decrease in the density $\rho_{w0}$ in the vicinity of the frontal critical point compared with its value in continuum flow.

Let us consider in greater detail the case of rarefied flow around a disk with Mach number M = 3.75-3.8 and Reynolds number $R_\infty$ varying in the limits $12 \leqslant R_\infty \leqslant 52$ (Figure 4). When $Re_\infty = 52$ the density profile breaks down quite clearly into two regions: the diffused front of the shock wave and a region of slower compression where the pressure gradient is small while the value of the pressure itself is slightly smaller than the value corresponding to continuum flow of a diatomic gas around a blunt body.

The mean free path of the molecules in the second region is substantially less than the dimension of the body, which makes it possible to assume that the flow here is close to continuum flow. The thickness of the boundary layer in the vicinity of the frontal critical point, computed by the method which is valid when $R_\infty = \infty$ [12], has a value of $0.4r^\circ$. This is substantially less than the thickness of the shock wave front. For practical purposes the shock wave and the boundary layer do not overlap.

We can conclude from Figure 4 that for flow with $R_\infty = 35$ and 24 the shock wave has filled the entire perturbed region in front of the disk and has

engulfed the boundary layer. The thickness and structure of the boundary layer cannot be computed by any known methods.

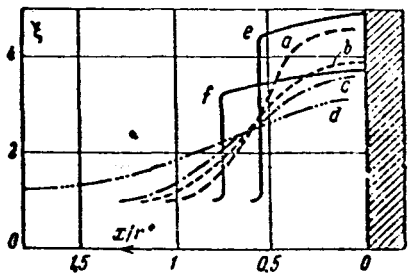


Figure 4. Flow Around a Disk at M = 3.75-3.8: a - $R_\infty$ = 52, b - $R_\infty$ = 35, c - $R_\infty$ = 24, d - $R_\infty$ = 12, e - $R_\infty$ = ∞, γ = 7/5, f - $R_\infty$ = ∞, γ = 5/3.

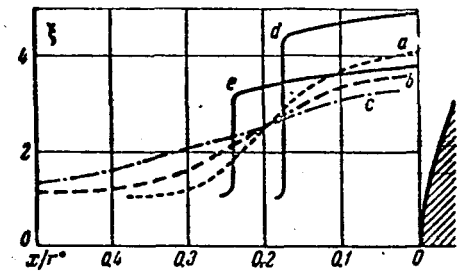


Figure 5. Flow Around a Sphere at M = 3.7-3.8: a - $R_\infty$ = 100, b - $R_\infty$ = 52, c - $R_\infty$ = 35, d - $R_\infty$ = ∞, γ = 7/5, e - $R_\infty$ = ∞, γ = 5/3.

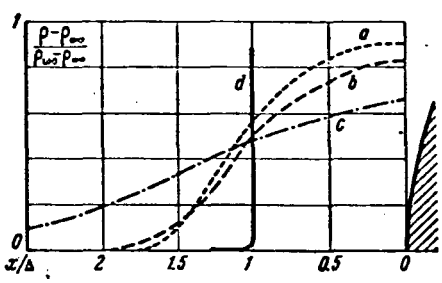


Figure 6. Flow Around a Sphere with $R_\infty$ = 90-100: a - M = 2.6, b - M = 3.7, c - M = 5.8, d - $R_\infty$ = ∞, γ = 7/5.

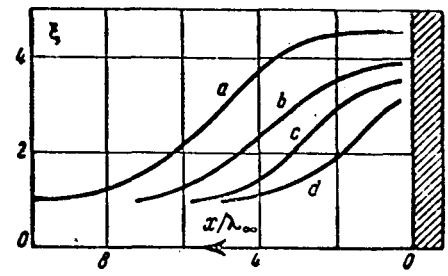


Figure 7. a - $R_\infty$ = 52, b - $R_\infty$= 35, c - $R_\infty$ = 24, d - $R_\infty$ = 12.

Indeed the structure of the boundary layer now depends to a great extent on processes in the shock wave which are characterized by the discrete nature of the medium and by large deviations from equilibrium. We can see from Figure 4 that when $R_\infty$ = 35 and 24 the measured value of the density $\rho_{w0}$ near the frontal critical point turns out to be close to the value which corresponds to continuum flow of a monotomic gas (γ = 5/3).

When $R_\infty$ = 12 the shock wave ahead of the blunt body disappears. The density profile characteristic of a shock wave is completely absent. Figure 7 shows the density profiles for the case of flow around a disk under consideration at M = 3.75-3.8 as a function of the distance $x/\lambda_\infty$ from the frontal critical point, reduced to the mean free path in the incident flow. A similar picture showing a change in the nature of flow when the density of the incident flux is decreased, is observed for the second and third series of experiments (Figures 5, 6). It is interesting to note that the disappearance of the shock

wave in front of the body is observed in all cases when the mean free path in /113
the incident flow $\lambda_\infty$ is approximately equal to the value of continuum detachment $\Delta$ of the shock wave from the corresponding body.

A more graphic picture concerning the evolution of the compressed layer in front of the blunt body may be obtained if its distance from the frontal critical point is expressed in terms of the local mean free path $\lambda(x)$. We introduce the variable

$$\eta = \int_0^x \frac{dx}{\lambda(x)} = \frac{1}{\lambda_\infty} \int_0^x \frac{\rho}{\rho_\infty} \frac{\Omega^{(22)*}(kT/\varepsilon)}{\Omega^{(22)*}(kT_\infty/\varepsilon)} dx \tag{3}$$

which represents the number of local mean free paths which can be arranged along the segment (0, x). The functions $\Omega^{(22)*}(KT/\varepsilon)$ in expression (3) are obtained when the viscosity coefficient is computed [7]. We may assume that the parameter gives a rough approximation of the number of collisions which a certain selected molecule undergoes on the average when transversing the path from point x to point x = 0. When equation (3) was used in the calculations it was assumed that the temperature T profile was similar to the experimental density profile

$$\frac{T - T_\infty}{T_0 - T_\infty} = \frac{\rho - \rho_\infty}{\rho_{x0} - \rho_\infty} \tag{4}$$

and experimental data presented in [7] for the Lennard-Jones potential were used to compute $\Omega^{(22)*}(KT/\varepsilon)$.

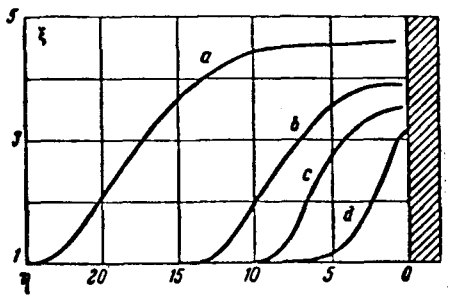


Figure 8. a - $R_\infty = 52$, b - $R_\infty = 35$, c - $R_\infty = 24$, d - $R_\infty = 12$.

The results of the processing experimental data for the case of flow around a disk for M = 3.75-3.8 and $12 \leqslant R_\infty \leqslant 52$ are shown in Figure 8.

An examination of Figure 8 enables us to conclude that when the flow becomes more rarefied the number of collisions experienced by a molecule as it passes through the perturbed layer in front of the body gradually decreases.

This effect will produce a situation where, after some moment of time, the internal degrees of freedom of the molecules arriving in the vicinity of the frontal critical point will not have enough time to adjust to the temperature of the forward motion. As the density is further decreased the translational degrees of freedom will also be unable to reach their equilibrium state.

Under our experimental conditions ($T_0 \approx 300°K$) only the translational and rotational degrees of freedom could be excited. Assuming that the latter are inert degrees of freedom and assuming also that the active translational degrees of freedom enter into complete equilibrium at the front critical point, we can find the state of the gas at this point in the case where the rotational temperature is completely frozen. The state of the gas in the receiver, in the incident flow and at the front critical point for such a flow may be expressed in the form of the double equality

$$c_p T_0 = c_{pt} T_\infty + c_{vr} T_\infty + {}^1/_2 u^2 = c_{pt} T_{w0} + c_{vr} T_\infty \tag{5}$$

Here u and $T_\infty$ are the velocity and temperature in the incident flow, $c_{pt}$ is the specific heat at constant pressure of the gas which has only translational degrees of freedom, $c_{vr}$ is the specific heat corresponding to the rotational degrees of freedom of a diatomic gas, $c_p = c_{pt} + c_{vr}$. It is also assumed in Expression (5) that the transition of the gas from the state in the receiver to the state in the incident flow is in equilibrium.

On the other hand, in the case of high density fluxes when the number of collisions is sufficiently large and rotation has time to relax to its equilibrium state, relation (5) has the form

$$c_p T_0 = c_{pt} T_\infty + c_{vr} T_\infty + {}^1/_2 u^2 = c_{pt} T_0 + c_{vr} T_0 \tag{6}$$

If we now combine the left and right sides of (5) and (6), substituting $c_{pt}$ and $c_{vr}$ by their numerical values, equal respectively to 5/2R and R (R is the gas constant), and disregard the quantity $c_{vr} T_\infty$ in the right side of (5) compared with $c_{vr} T_0$ we find that the gas temperature in the vicinity of the front critical point of the blunt body $T_{w0}$ exceeds the stagnation temperature $T_0$ by a factor 1.4 if the rotational degrees of freedom are frozen. When the density of the incident flux is increased the rotational degrees of freedom /114
become excited when they pass the compressed layer in front of the body and the temperature $T_{w0}$ begins to approach the temperature $T_0$. Finally, for continuum flow $T_{w0} = T_0$. The variation in temperature $T_{w0}$ in the vicinity of the front critical point of the blunt body during changes in the density of the incident

flux may be established by using the equation of state $p_{w0} = R\rho_{w0}T_{w0}$ and the values of $P_{w0}$ measured in our experiments, or the measurements of $P_{w0}$ obtained by the total pressure attachment [8]. The latter work was carried out in the same wind tunnel with the same nozzles as used in our tests. The attachments have the form of spheres and cylinders with a flat end. The $R_\infty$ number in this work was computed from the diameter of the attachment $2r^0$ and from the viscosity established from the Sutherland's model with the constant C = 114. For our purposes, these $R_\infty$ numbers were recomputed in accordance with the Lennard-Jones model and reduced to the radius $r^0$. After this the known values of $P_{w0}$ and $P_{w0}$ for the same M and $R_\infty$ were used to determine the temperatures $T_{w0}$ at the front critical point of the body. The results corresponding to all experiments shown in the table are represented in Figure 9 as a function $T = T_{w0}/T_0$ of the ratio $\Delta/\lambda\infty$. We can see from this figure that the ratio $T_{w0}/T_0$ both for the disk and for the sphere has approximately the same value in the investigated range of Knudsen number where $\Delta/\lambda\infty$ is the same. It is interesting to note that the correction in [8] to the readings of the total pressure attachments displays the same behavior.

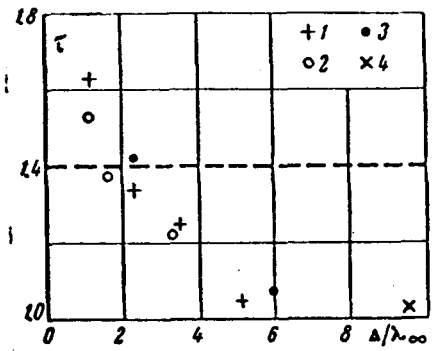


Figure 9. 1 - First Series of experiments (table); 2- Second Series of Experiments (table); 3 - Third Series of Experiments (table); 4 - Experiment for Flow Around the Disc at M = 6, $R_\infty$ = 170 (see [3]).

An increase in $T_{w0}/T_0$ during a decrease in the parameter $\Delta/\lambda\infty$ is associated with a delay in the establishment of equilibrium in rotational and translational degrees of freedom. When $\Delta/\lambda\infty \approx 2$ the experimental value of $T_{w0}/T_0$ turns out to be equal to the corresponding value in a flow with frozen rotational degrees of freedom. However, this result apparently has no absolute meaning. Indeed the translational degrees of freedom cease to be established somewhat earlier when $\Delta/\lambda\infty \geqslant 2$ while the rotational degrees of freedom, in turn, continue to be excited even when $\Delta/\lambda\infty \leqslant 2$. Flow with a delay in the

rotational degrees of freedom when the translational degrees of freedom are established, takes place somewhat earlier, somewhere in the region $3 < \Delta/\lambda_\infty \leqslant 10$.

When $\Delta/\lambda_\infty < 2$ the determination of temperature $T_{w0}$ by the formal application of the equations of state becomes invalid. The increase in the quantity $T_{w0}/T_0$ in this region above the value of 1.4 established above is explained by the fact that $T_{w0}$ actually contains the kinetic energy of the mass movement and this energy is no longer equal to zero in the vicinity of the front critical point. Furthermore the state of the gas here depends substantially on the nature of the molecular reflection from the surface. Therefore the points in Figure 9 obtained from the experiments for $\Delta/\lambda_\infty < 2$ should be considered only from a qualitative standpoint.

In summarizing the investigation we can maintain that an increase in the thickness of the detached shock wave in front of a blunt body, when the density of the incident flow is lowered, leads to the beginning of relaxation effects in the compressed gas layer ahead of the body. As the gas is further rarefied the shock wave in front of the body disappears and a state of free molecular flow occurs. The relation $\Delta \approx \lambda_\infty$ establishes the point at which the shock wave disappears. The ratio of the continuum shock wave detachment distance $\Delta$ from the body to the mean free path in the incident flow $\lambda_\infty$ may be considered as the flow criterion before the shock wave disappears. A stricter criterion is the number of collisions experienced by a given molecule as it passes through the perturbed layer in front of the blunt body.

The author is grateful to G. I. Petrov and V. S. Avduyevskiy for their consideration of the results of this work and to V. G. Voytichenko and Z. A. Barikov for their assistance in carrying out the experiments.

## REFERENCES

1. Hurlbut, F. C., Electron Beam Density Probe for Measurement in Rarefied Gas Flow, J. Appl. Phys., Vol. 30, No. 3, p. 273, 1959.
2. Ivanov, A. V., *Eksperimental'noye opredeleniye raspredeleniya plotnosti pered zatuplennymi telami, obtekaemymi sverkhzvukovym potokom razrezchnnogo gaza,* [Experimental Determination of Density Distribution in Front of Blunted Bodies in a Supersonic Rarefied Gas Flow], PMTF, No. 6, p. 99, 1964.
3. Ivanov, A. V., *Struktura udarnoy volny v vozdukhe pri chislakh M ot 2.6 do 6,* [The Structure of the Shock Wave in Air at Mach Numbers 2.6 to 6], Izb. AN SSSR, MZhG, No. 1, 1967.
4. Linzer, M., D. F. Horning, Structure of Shock Fronts in Argon and Nitrogen, Phis. Fluids, Vol. 6, No. 12, p. 1661, 1963.
5. Robben, F., L. Talbot, Measurement of Shock Wave Thickness by the Electron Beam Fluorescence Method, Phis. Fluids, Vol. 9, No. 4, p. 633, 1966.
6. Probstein, R. F., Continuum Theory and Rarefied Hypersonic Aerodynamics, Rarefied Gas Dynamics, p. 416 (Proc. of the First Intern. Symposium Held

at Nice).
7. Girshfel'der Dzh, Kertis Ch., R. Berd, *Molekulyarnaya teoriya gazov i zidkostey*, [The Molecular Theory of Gases and Liquids], Foreign Literature Press, pp. 416, 868.
8. Sukhnev, V. A., *Ob opredelenii popravok k pokazaniyam nasadkov polnogo napora v sverkhzvukovom potoke razrezhennogo gaza*, [On the Determination of Corrections to the Total Pressure Attachment Readings in the Supersonic Flow of Rarefied Gas], Izv. SSSR, Mekhanika i mashinostroyeniye, No. 5, p. 161, 1964.
9. Sherman, P. M., Visualization of Low Density Flow by Means of Oxygen Absorbtion of Ultraviolet Radiation, J. Aeronaut. Sci., Vol. 24, No. 2, p. 93, 1957.
10. Ladenburg, R., V. Lewis, R. Pierce, Editors, *Fizicheskiye izmereniya v gazovoy dinamike i pri gorenii*, [Physical Measurements in Gas Dymanics During Combustion], Foreign Literature Press, 1957.
11. Kogan, M. N., *O giperzvukovykh techeniyakh razrezhennogo gaza*, [On the Hypersonic Flows of a Rarefied Gas], PMM, Vol. 26, No. 3, p. 520, 1962.
12. Avduyevskiy, V. S., R. M. Kopyatkevich, *Raschet laminarnogo pogranichnogo sloya v szhimayemom gaze pri nalichii teploobmena i proizvol'nom raspredelenii davleniya vdol' poverkhnosti*, [The Computation of the Laminar Boundary Layer in a Compressed Gas in the Presence of Heat Transfer and with an Arbitrary Distribution of Pressure Along the Surface], Izv. AN SSSR, OTM, Mekhanika i mashinostroyeniye, No. 1, 1960.

Translated for the National Aeronautics and Space Administration under Contract No. NASw-1695 by Techtran Corporation, P. O. Box 729, Glen Burnie, Maryland, 21061.